Grain refinement of commercial pure Al treated by Pulsed Magneto-Oscillation on the top surface of melt

Dong Liang[1], Zhu-yuan Liang[1], Jie Sun[1], *Qi-jie Zhai[1], Wang Gui [2], and David H. StJohn[2]

1. Shanghai Key Laboratory of Modern Metallurgy & Materials Processing, Shanghai University, Shanghai 200072, China;

2. Centre for Advanced Materials Processing and Manufacturing, The University of Queensland, Queensland 4072, Australia

Abstract: Commercial pure Al can be refined by Pulsed Magneto-Oscillation (PMO) treatment applied via a plate induction coil above the top surface of the melt. The proportion of the equiaxed zone area increases with decreasing Height to Diameter (H/D) ratios from 3.5 to1.8 and further to 1.0. Meanwhile, it increases and then decreases with increasing peak current for the three kinds of ingots with H/D ratios of 3.5, 1.8 and 1.0, respectively. However, when the H/D ratio decreases to 0.44, the area proportion of equiaxed zone can reach the maximum value with a lower peak current. FEA software simulation indicates that smaller H/D ratio results in larger current density, electromagnetic force and convection on the top surface of the melt, favoring nucleation and subsequent grain formation. Through evaluating Joule heating effect by PMO, it was found that the proper amount of Joule heating benefits grain refinement. Excessive Joule heating can reduce the size of the equiaxed zone and change the growth morphology of the grains.

Key words: grain refinement; casting process; nucleation and growth; finite element (FE) simulation; pulsed magneto-oscillation (PMO)

CLC numbers: TG146.21 **Document code:** A **Article ID:** 1672-6421(2015)01-048-06

Using a magnetic field to stimulate nucleation and promote grain formation in the bulk of the liquid metal has been considered an effective way to improve the as-cast macrostructure of materials [1-3]. The technique has attracted increasing interest because there is no need for external materials to be immersed into the melts, and therefore no new contaminations are introduced compared to other techniques such as ultrasonic treatment [4] and mechanical vibration [5].

It has been reported that a strong Pulsed Magnetic Field, referred to as PMF, can significantly refine the macrostructure of aluminum alloys [6-8]. The major drawback for PMF is its narrow operating window because the solidified structure cannot be refined with a low PMF power and when the PMF power is set too high, the melt may spatter to an unacceptable level [9-10]. In order to overcome this barrier, a successful modification of PMF was made by narrowing the pulse width and reducing the pulsed current of the output power, which led to a promising technique called the Pulsed Magneto-Oscillation (PMO) technique [10]. This technique induces a magnetic field only in the surface regions of the melt rather than throughout the melt. It has been demonstrated that the PMO can be much more easily applied in an industrial environment compared to any other electromagnetic techniques [10]. However, in previous studies, a coil with a spiral configuration was normally placed around the ingot or casting, but when the casting size is large, it is not practical to apply the PMO. More recently, in order to break through this limitation on the induction coil, Yin et al. [11] introduced a designed plate coil placed just above the top surface of the melt and successfully achieved significant refinement of the as-cast macrostructure. Even though very promising results have been reported [11], there is still a lack of understanding of the effect of the shape of the casting/ingot mold on the refinement of the macrostructure.

The present work investigated the effect of PMO using a plate coil acting on the top surface of the melt on the grain refinement of commercial pure Al with particular focus on the peak current of PMO and the

* Qi-jie Zhai

Male, born in 1959, Ph.D, Professor. Research interests: metal solidification and microstructure refinement.

E-mail: qjzhai@shu.edu.cn

Received: 2014-09-10; Accepted: 2014-11-11

ratio of the Height to Diameter (H/D) of the casting/ingot mold. For this purpose, various peak currents were applied to the melt which was cast into molds with a range of H/D ratios. The physical factors such as current intensity, electromagnetic force, and induced convection were simulated by FEA software, and the effect of the amount of Joule heating generated by PMO was also evaluated.

1 Experimental procedure and FEA modeling

1.1 Experimental procedure

Commercial pure aluminum (99.7wt%) was melted in an electric resistance furnace and held at 1,023 K for 30 min. The melt was then poured into four sand molds with a cylindrical cavity with the dimension of Φ40 mm × 140 mm, Φ50 mm × 90 mm, Φ60 mm × 62 mm, and Φ80 mm × 35 mm, respectively. These mold cavities were designed to have an equal volume of 176 cm^3, but with different H/D ratios: 3.5, 1.8, 1.0 and 0.44, respectively. After pouring, the plate induction coil was placed above the top of the sand mold and the PMO generator was immediately turned on. PMO treatment was applied until the melt completely solidified. The detail of the experimental apparatus has been reported elsewhere by the current authors [11]. In this study, the peak of the PMO current was set respectively to 100k_i A, 150k_i A and 200k_i A, while the frequency was kept at 25h_i Hz for all the experiments, where k_i and h_i are constant coefficients of the pulse generator. The solidified samples were sectioned along the vertical axis through the center of the casting and the macrostructures of the cast samples were prepared and characterized using standard metallographic procedures. The fraction of the equiaxed zone was determined by Image-Pro Plus software over the acquired metallographic images.

1.2 FEA modeling

In order to understand the effect of the current density, electomagnetic force and convection induced by the PMO treatment in the experimental conditions, numerical simulation was conducted using the commerical FEA package ANSYS.

(a) Electromagnetic field model

The derived Maxwell equations can be expressed as the following equations (1–4):

$$\nabla \times \boldsymbol{E}(\boldsymbol{r},t) = -\partial \boldsymbol{B}(\boldsymbol{r},t)/\partial t \quad (1)$$

$$\nabla \times \boldsymbol{B}(\boldsymbol{r},t) = \mu \boldsymbol{J} + \mu\varepsilon(\partial \boldsymbol{E}(\boldsymbol{r},t)/\partial t) \quad (2)$$

$$\nabla \cdot \boldsymbol{E}(\boldsymbol{r},t) = \rho/\varepsilon \quad (3)$$

$$\nabla \cdot \boldsymbol{B}(\boldsymbol{r},t) = 0 \quad (4)$$

where, $\boldsymbol{E}$ is electric field intensity vector, $\boldsymbol{B}$ is magnetic induction intensity vector, $\boldsymbol{J}$ is current density vector, ε is dielectric constant, μ is magneto permittivity, $\boldsymbol{r}$ is displacement vector, and t is time.

The relationships between the boundary values of the electromagnetic field are derived by equations (5–8):

$$\boldsymbol{n}\cdot(\boldsymbol{D_2}-\boldsymbol{D_1})=\sigma \quad (5)$$

$$\boldsymbol{n}\times(\boldsymbol{E_2}-\boldsymbol{E_1})=0 \quad (6)$$

$$\boldsymbol{n}\times(\boldsymbol{E_2}-\boldsymbol{E_1})=0 \quad (7)$$

$$\boldsymbol{n}\times(\boldsymbol{H_2}-\boldsymbol{H_1})=\alpha \quad (8)$$

where, $\boldsymbol{n}$ is per unit normal vector, σ in equation (5) is electric charge intensity, and α is surface current density, $\boldsymbol{D}$ is electric displacement vector, $\boldsymbol{H}$ is magnetic field intensity vector.

The electromagnetic force induced by PMO on the top surface of the melt can be described using equations (9) and (10)

$$f_x(I_0,r,t) = J \cdot B_y = k_y(r,\varphi_2(r))k'(r,\varphi(r))I_0{}^2T(t,\varphi_2(r))T(t,\varphi(r)) \quad (9)$$

$$f_y(I_0,r,t) = -J \cdot B_x = -k_x(r,\varphi_1(r))k'(r,\varphi(r))I_0{}^2T(t,\varphi_1(r))T(t,\varphi(r)) \quad (10)$$

where, f_x is electromagnetic force which is parallel to the liquid surface, f_y is electromagnetic force which is perpendicular to the liquid surface, k_y, k' and k_x are coefficients, I_0 is the pulse peak current, and T is time coefficient.

When the air boundary layer is zero, the electrical parameters of the materials are presented in Table 1 [12].

Table 1: Electrical parameter of materials

	Electrical resistivity (Ωm)	Relative permeability
Aluminum (660 ℃)	2.4×10^{-7}	1
Copper (25 ℃)	1.7×10^{-8}	1
Air (25 ℃)	…	1

(b) Fluid convection model

The continuity equation and the momentum balance equation are the basic expressions of fluid mechanics. The continuity equation is shown as equation (11), and the momentum balance equation is described in equation (12) [13]:

$$\frac{\partial \rho}{\partial \tau} + \frac{\partial(\rho v_x)}{\partial x} + \frac{\partial(\rho v_y)}{\partial y} + \frac{\partial(\rho v_z)}{\partial z} = 0 \quad (11)$$

$$\begin{aligned}
&\frac{\partial(\rho v_x)}{\partial \tau} + \frac{\partial(\rho v_x v_x)}{\partial x} + \frac{\partial(\rho v_y v_x)}{\partial y} + \frac{\partial(\rho v_z v_x)}{\partial z} \\
&= \frac{\partial}{\partial x}\left(\mu_e \frac{\partial v_x}{\partial x}\right) + \frac{\partial}{\partial y}\left(\mu_e \frac{\partial v_x}{\partial y}\right) + \frac{\partial}{\partial z}\left(\mu_e \frac{\partial v_x}{\partial z}\right) - \frac{\partial p}{\partial x} + \rho g_x \\
&\frac{\partial(\rho v_y)}{\partial \tau} + \frac{\partial(\rho v_x v_y)}{\partial x} + \frac{\partial(\rho v_y v_y)}{\partial y} + \frac{\partial(\rho v_z v_y)}{\partial z} \\
&= \frac{\partial}{\partial x}\left(\mu_e \frac{\partial v_y}{\partial x}\right) + \frac{\partial}{\partial y}\left(\mu_e \frac{\partial v_y}{\partial y}\right) + \frac{\partial}{\partial z}\left(\mu_e \frac{\partial v_y}{\partial z}\right) - \frac{\partial p}{\partial y} + \rho g_y \\
&\frac{\partial(\rho v_z)}{\partial \tau} + \frac{\partial(\rho v_x v_z)}{\partial x} + \frac{\partial(\rho v_y v_z)}{\partial y} + \frac{\partial(\rho v_z v_z)}{\partial z} \\
&= \frac{\partial}{\partial x}\left(\mu_e \frac{\partial v_z}{\partial x}\right) + \frac{\partial}{\partial y}\left(\mu_e \frac{\partial v_z}{\partial y}\right) + \frac{\partial}{\partial z}\left(\mu_e \frac{\partial v_z}{\partial z}\right) - \frac{\partial p}{\partial z} + \rho g_z
\end{aligned} \quad (12)$$

where, ρ is the density of the melt, p is the external pressure, g_i is the acceleration due to gravity, and μ_e is the effective coefficient of viscosity.

The boundary conditions are as follows [14]:

Symmetrical axis $v_x = 0$; the bottom and the wall of the mold $v_x = 0$, $v_y = 0$;

The top surface of the melt $v_y = 0$.

The parameters of the commercially pure Al melt are listed in Table 2, which is from the commercial casting process simulation software PROCAST [15] and reference [16].

Table 2: Physical parameters of pure aluminum (665 °C)

	Density ($kg \cdot m^{-3}$)	Viscosity ($Pa \cdot S$)	Thermal conductivity ($Wm^{-1} \cdot K^{-1}$)
Aluminum	2375	2.5×10^{-3}	2112

2 Results and discussion

2.1 Grain structure

Figure 1 shows the as-cast grain structure of the ingots with H/D ratios of 3.5, 1.8, and 1.0 and treated with different PMO peak currents: 0 A (i.e. no PMO treatment), $100k_i$ A, $150k_i$ A, and $200k_i$ A. Typical columnar dendritic grains were formed horizontally throughout the sample without PMO treatment as shown in Fig. 1(a1, b1, c1), and equiaxed dendrites were found at the bottom of the ingots. With PMO, the refined equiaxed grains appeared at the central and the bottom regions of the ingots. Figure 1 (a2-a3, b2-b3, c2-c3) shows that the size of the equiaxed zone firstly increases with increasing PMO peak current. However, when the peak current was too high ($200k_i$ A), the size of the equiaxed zone decreased, as shown in Fig. 1(a4, b4, c4).

The sizes of the equiaxed zones in ingots with different H/D ratios and peak currents are shown quantitatively in Fig. 2. It can be seen that the size of the equiaxed grain zone first increases, and then decreases after the peak current was higher than $150k_i$ A for all the three ingots. It is also seen that for each peak current value, the size of the equiaxed grain zone increases with decreasing H/D ratio. It is clear that the H/D ratio has a significant impact on the overall grain structure of the ingots from Fig. 1 and Fig. 2. The effect of the H/D ratio can be explained by the current intensity, Lorentz force induced by PMO, and the forced convection as discussed in sections 2.2 and 2.3.

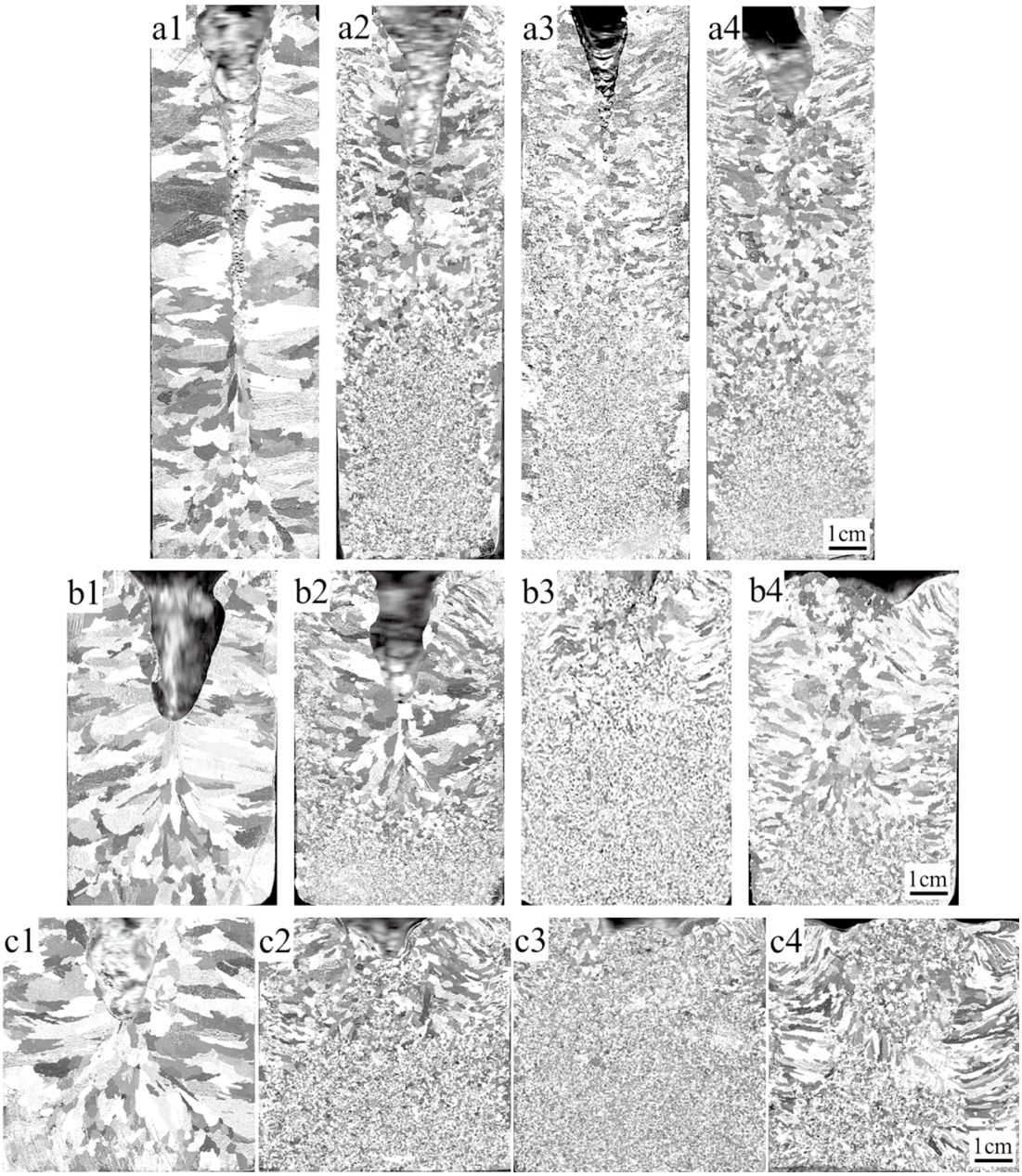

Fig. 1: Macrostructures of ingots with H/D of (a) 3.5, (b) 1.8, and (c) 1.0 under different PMO peak currents: (1) 0 A, (2) $100k_i$ A, (3) $150k_i$ A, (4) $200k_i$ A

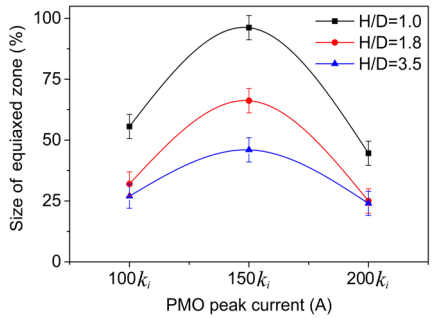

Fig. 2: Fraction of equiaxed grains *vs* H/D with various peak currents

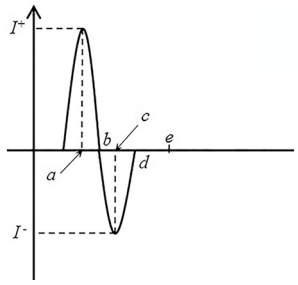

Fig. 3: Schematic sketch of a current pulse with different moments

2.2 FEA simulation

Figure 3 shows the different moments of a whole current pulse with the whole pulse comprising five key moments. In this work, the induced current intensity, Lorentz force and flow field of the ingots with H/D ratios of 3.5 and 1.0 were simulated at the same moment "*a*" and the same peak current of 150k_i A.

Figure 4a1 and Fig. 4b1 reveal that the induced current intensity at the surface of the ingot with H/D = 1.0 is about 1.5 times larger than that in the ingot with H/D = 3.5. Figures 4b2 and 4a2 show the electromagnetic force at the surface of melt (H/D = 1.0) is about 3.5 times greater than that of the melt with an H/D ratio of 3.5. It can be expected that the greater the induced electromagnetic force on the melt surface, the more vigorous the convection in general. Figures 4b3 and 4a3 show that the largest convection velocity in the melt (H/D = 1.0) is about 2 times higher than that in the melt with H/D = 3.5.

The simulation results indicate a larger surface area and greater current intensity, which favor the nucleation near the top surface of the melt. As a result, the number of grains formed near the top surface would increase with a decrease in the H/D ratio. Meanwhile, the electromagnetic force induced by PMO promotes the formation of nuclei near the top surface, which then drift into the bulk melt. In addition, the electromagnetic force intensifies convection within the melt, which causes the grains to move from the top surface drifting towards the

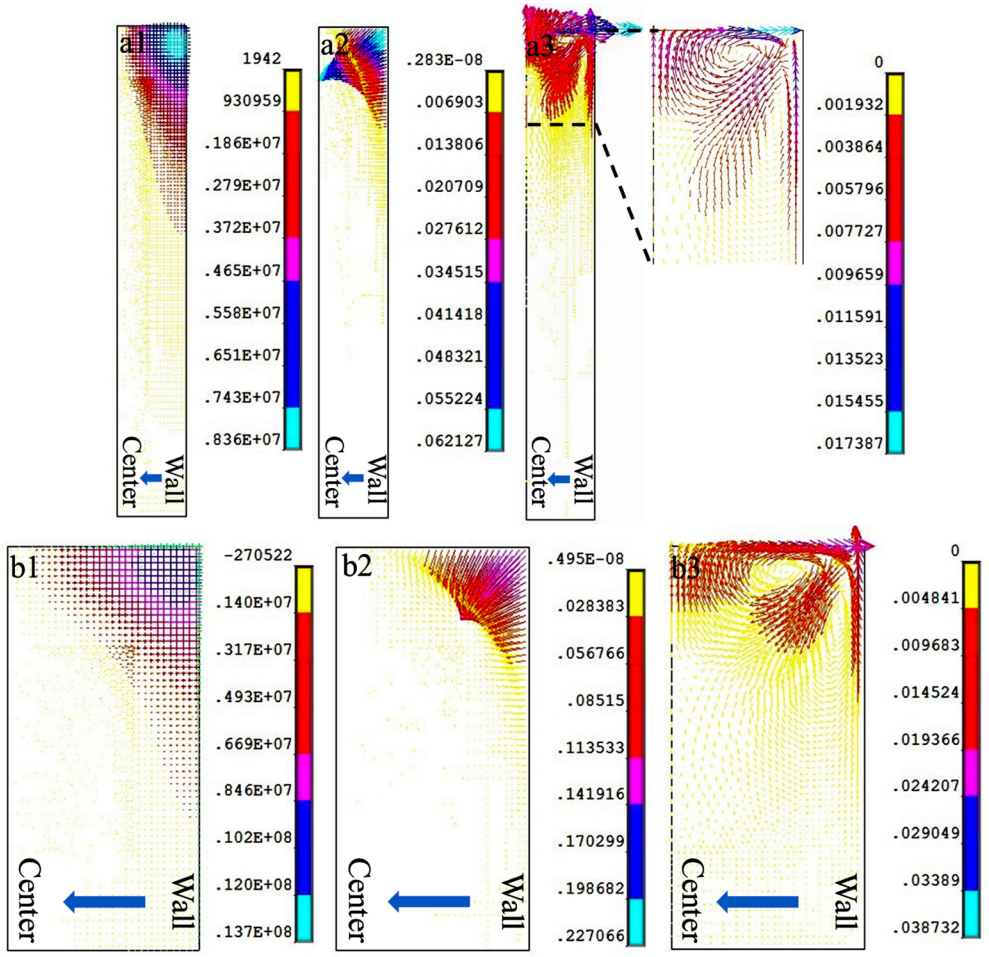

Fig. 4: Distribution of current density (1), electromagnetic force (2) and flow field (3) of ingot with H/D 3.5 (a) and 1.0 at the peak current of 150k_i A (b)

center of the melt [11]. The forced convection of the melt is also important to the grain refinement of metals, because vigorous convection of the melt makes the temperature field more uniform, favoring the formation and survival of grains. Dong et al. [17] also identified this mechnism in a study of the PMO treatment. Therefore, when treated with the same PMO peak current, the smaller the H/D ratio, the larger the size of the equiaxed zone, as shown in Fig. 2.

2.3 Effect of peak current and Joule heating on refinement

It has been shown that the value of peak current plays a critical role in refining the macrostructure. Apart from the electromagnetic force and convection induced by PMO, the effect of the PMO treatment also induces Joule heating which is associated with the current intensity on the top surface of the melt. This Joule heating is mainly concentrated in the top surface zone and can change the temperature distribution in the surface area, therefore affecting the degree of grain refienment. Joule heating can be determined by equation (13)

$$Q = f \cdot l \int_0^R 2\pi R dR \int_0^{T_l} J^2(I_0, r, t)\sigma dt \quad (13)$$

where, f is the discharging frequency, l is the length of electromagnetic field existing in the melt, R is the radius of the melt, J is the current density, r is the coordinates in space, T_1 is one pulse period, and σ is the liquid resistivity.

According to equation (13), Joule heating is proportional to the square of the current density and the radius of the top surface of the melt. On the basis of the discussion above, the larger the surface area, the more Joule heating can be generated at the top surface of the melt. An appropriate level of the Joule heating can result in slightly prolonging the nucleation stage where more nucleated grains can be formed. However, if too much Joule heating is generated, then the surface zone of the melt will be kept at a higher temperature. On one hand, most of the nuclei cannot form near the top surface. On the other hand, the nuclei that are formed near the top surface will remelt in superheated surroundings. Therefore, when the peak current is too high, a high level of Joule heating can reduce the amount of refinement. For example, when the peak current reached $200k_i$ A, the refinement effect was significantly reduced for all three ingots (H/D = 3.5,1.8 and 1.0).

In order to further comprehensively investigate the effect of Joule heating on the grain refinement, an additional casting with a larger top surface and smaller height with H/D = 0.44 was cast, and the macrostructure of the ingot with the same level of the peak current as that in Fig. 1 is shown in Fig. 5. Without PMO treatment, the coarse columnar grains were growing simultaneously from both the lateral wall and the bottom of the mold, as seen in Fig. 5a. With the PMO treatment at the peak current of $100k_i$ A, an almost fully refined equiaxed grain structure could be formed as shown in Fig.

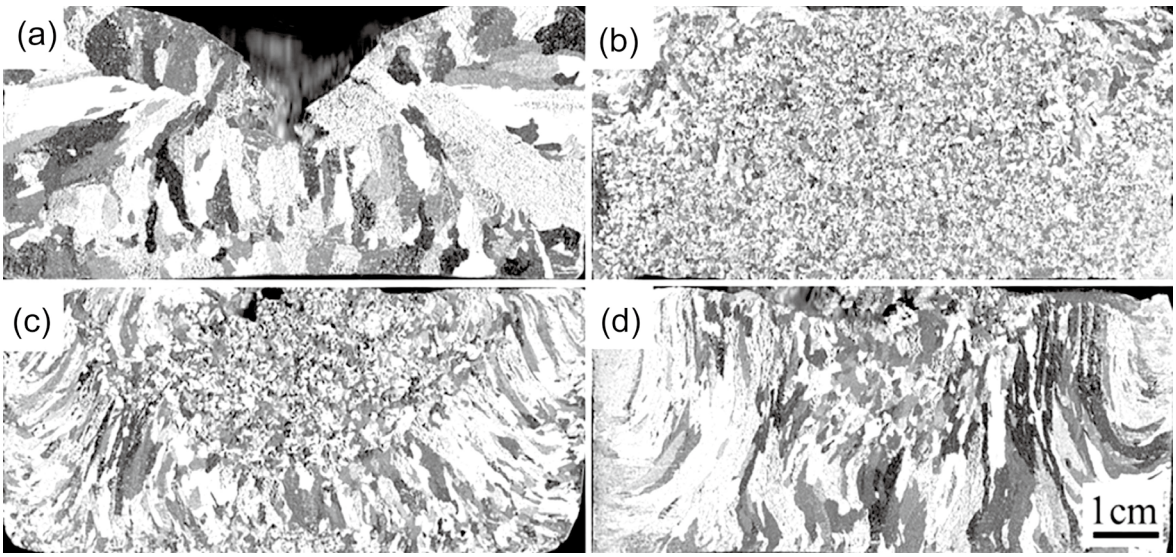

Fig. 5: Macrostructure of ingot with H/D= 0.44 under different PMO peak currents: (a) 0 A, (b) $100k_i$ A, (c) $150k_i$ A, (d) $200k_i$ A

5b, but with an increase in the PMO peak current from $100k_i$ A to $150k_i$ and further to $200k_i$ A, the size of the equiaxed zone decreased dramatically from 93% to 33% and 18%, respectively. Meanwhile, in the macrostructures of the ingot treated with a peak current of $200k_i$ A, the columnar crystals grew from the bottom to the top surface like the structure under directional solidification conditions, and the horizontal columnar grains were suppressed completely, revealing that the Joule heating has an important effect on the grain refinement of commercial pure Al castings.

3 Conclusions

(1) The pulsed Magneto-Oscillation treatment has a significant impact on the grain refinement of commercial purity aluminum ingots. There is an optimum value for the peak current in order to achieve good refinement. By decreasing the Height to Diameter ratio of the ingot, a larger equiaxed zone can be obtained. When the H/D ratio decreases to 0.44, a smaller peak current is needed to obtain the best refined solidification structure.

(2) The induction current, electromagnetic force and forced convection all increase with an increase in area of the top surface of the melts. The induction current is a pivotal factor for triggering nucleation. Electromagnetic force and induced convection favor the survival of the grains.

(3) Joule heating generated by the PMO treatment also has an important effect on the nucleation and formation of grains. It should be controlled within an appropriate range to obtain the optimum size of the equiaxed zone.

References

[1] Li Qiushu, Song Changjiang, Li Hanbin, et al. Effect of pulsed magnetic field on microstructure of 1Cr18Ni9Ti austenitic stainless steel. Materials Science and Engineering A, 2007, 466: 101–105.

[2] Liao Xiliang, Zhai Qijie, Luo Jun, et al. Refining mechanism of the electric current pulse on the solidification structure of pure aluminum. Acta Materialia, 2007, 55: 3103–3109.

[3] Pei Ning, Gong Yongyong, Li Renxing, et al. Mechanism of pulse magneto oscillation grain refinement on pure Al. China Foundry, 2011, 8: 47–50.

[4] Ramirez A, Ma Q, Davis B. et al. Potency of high-intensity ultrasonic treatment for grain refinement of magnesium alloys. Scripta Materialia, 2008, 59: 19–21.

[5] Flemings M C, Riek R G, Young K P. Rheocasting. Materials Science and Engineering, 1976, 25: 103–107.

[6] Ma Xiaoping, Li Yingju, Yang Yuansheng. Grain refinement effect of pulsed magnetic field on solidified microstructure of superalloy IN718. Journal of Materials Research, 2009, 24: 3174–3181.

[7] Zhang L, Li W, Yao J P. Microstructures and thermal stability of the semi-solid 2024 aluminum alloy prepared using the pulsed magnetic field process: Effects of technological parameters. Journal of Alloy and Compound, 2013, 554: 156–161.

[8] Gao Yulai, Li Qiushu, Gong Yongyong, et al. Comparative study on structural transformation of low-molten metaling pure Al and high-molten metaling stainless steel under external pulsed magnetic field. Materials Letters, 2007, 61: 4011–4014.

[9] Fu J W, Yang Y S. Microstructure and mechanical properties of Mg-Al-Zn alloy under a low-voltage pulsed magnetic field. Materials Letters, 2012, 67: 252–255.

[10] Gong Yongyong, Luo Jun, Jing Jinxian, et al. Structure refinement of pure aluminum by pulse magneto-oscillation. Materials Science and Engineering A , 2008, 497: 147–152.

[11] Yin Zhenxing, Gong Yongyong, Li Bo, et al. Refining of pure aluminum cast structure by surface pulsed magneto-oscillation. Journal of Materials Processing Technology, 2012, 212: 2629–2634.

[12] Shimoji M, Itami T. 3.4 Electrotransport. Defect and Diffusion Forum, 1986: 216–219.

[13] Cheng Yufeng. The Simulation Research of Electromagnetic Field, Flow Field, and Temperature Field Based on Finite Element Method. Master thesis, Shanghai University, 2013. (in Chinese)

[14] Ma Xiaoping, Yang Yuansheng and Wang Bin. Effect of pulsed magnetic field on superalloy melt. International Journal of Heat and Mass Transfer, 2009, 52: 5285–5292.

[15] ProCast User Manual Version 2010. 1. ESI group. The Virtual Try-out Space Company, 2010.

[16] Bian Maoshu, Chen Qiu and Wang Jingtang. Density surface tension wettability and adhesive power of liquid Al and Al-RE alloy on BN surface. Acta Metall Sin, 1988, 24: 139–141.

[17] Liang Dong, Liang Zhuyuan, Zhai Qijie, et al. Nucleation and grain formation of pure Al under pulsed magneto-oscillation treatment. Materials Letters, 2014, 130: 48–50.

This research was financially supported by the National Natural Science Foundation of China (Grant No. 51320105003), the Australian Research Council Centre of Excellence for Design in Light Metals and, ARC Discovery Project DP140100702 and the ExoMet Project co-funded by the European Commission's 7th Framework Programme (Contract FP7-NMP3-LA-2012-280421).